**Proceedings Paper:**
Delis, I, Hilt, P, Pozzo, T et al. (2 more authors) (2018) Characterization of whole-body muscle activity during reaching movements using space-by-time modularity and functional similarity analysis. In: Proceedings of the 10th Hellenic Conference on Artificial Intelligence. SETN 2018: 10th Hellenic Conference on Artificial Intelligence, 09-12 Jul 2018, Patras, Greece. ACM . ISBN 978-1-4503-6433-1

https://doi.org/10.1145/3200947.3201006

# Characterization of whole-body muscle activity during reaching movements using space-by-time modularity and functional similarity analysis

Full Paper

Ioannis Delis
Department of Biomedical Sciences
University of Leeds
Leeds, LS2 9JT, UK
i.delis@leeds.co.uk

Pauline Hilt
Fondazione Istituto Italiano di Tecnologia, Centro di Neurofisiologia traslazionale c/o sezione Fisiologia Umana
44121 Ferrara, Italy
pauline.hilt@iit.it

Thierry Pozzo
Fondazione Istituto Italiano di Tecnologia, Centro di Neurofisiologia traslazionale c/o sezione Fisiologia Umana
44121 Ferrara, Italy
thierry.pozzo@iit.it

Stefano Panzeri
Neural Computation Laboratory, Center for Neuroscience and Cognitive Systems@unitn, Istituto Italiano di Tecnologia, 38068 Rovereto (TN), Italy
stefano.panzeri@iit.it

Bastien Berret
Univ. Paris-Sud, Université Paris-Saclay, 91405 Orsay Cedex, France
bastien.berret@u-psud.fr

## ABSTRACT

Voluntary movement is hypothesized to rely on a few low-dimensional structures, termed muscle synergies, whose recruitment translates task goals into effective muscle activity. However, the relationship of the synergies with the characteristics of the performed movements remains largely unexplored. To address this question, we recorded a comprehensive dataset of muscle activity during a variety of whole-body pointing movements. We decomposed the electromyographic (EMG) signals using a space-by-time modularity model which encompasses the main types of synergies. We then used a task decoding and information theoretic analysis to probe the role of each synergy by mapping it to specific task parameters. We found that the temporal and spatial aspects of the movements were encoded by different temporal and spatial muscle synergies, respectively, indicating that the identified synergies are tailored with complementary roles to account for the major movement attributes. This approach led to the development of a novel computational framework for comparing muscle synergies from different datasets according to their functional role. This functional similarity analysis yielded a small set of temporal and spatial synergies that describes the main features of whole-body reaching.

## KEYWORDS

Motor modularity, muscle synergies, EMG, space-by-time decomposition, whole-body movement, task decoding, functional similarity analysis.

## 1 INTRODUCTION

Human motor control has been hypothesized to rely on a limited set of building blocks, termed muscle synergies, motor primitives or more generically modules [1-5]. A key assumption of this hypothesis is that, in order to generate and execute movement, the central nervous system (CNS) selectively codes motor task parameters via the activation of certain muscle synergies [6]. This recruitment of muscle synergies gives rise to genuine muscle patterns that allow achievement of the desired motor task [7, 8]. However, much less is known about why synergies turn out to take specific forms, whether they are shaped to serve any specific motor function and if their structure depends on their functional role. To



SETN '18, July 9–15, 2018, Rio Patras, Greece

ACM ISBN 978-1-4503-6433-1/18/07…$15.00
https://doi.org/10.1145/3200947.3201006

address these questions, we probe the encoding of various movement features within distinct muscle synergies.

Here, we rely on a modularity model that separates the spatial and temporal aspects of muscle patterns. We combine this model with the collection of a remarkably large electromyographic (EMG) dataset (30 muscles) during performance of a rich set of whole-body movements, serving to decipher the dependence of modular structures on various task features.

We employ a multivariate decoding analysis that maps each synergy to a specific task parameter and allows dissecting the functional role of each synergy and quantifying its distinct contribution to the representation of task parameters. We then capitalize on this approach to compare synergies between different subjects based on their functional role as represented by the task parameters they encode rather than based on their muscle activation profile, which may vary significantly across subjects [9, 10]. Hence, we propose a novel functional similarity analysis that serves to cluster synergies across individuals. Ultimately, our results provide new insights into the functional interpretation of spatial and temporal muscle synergies.

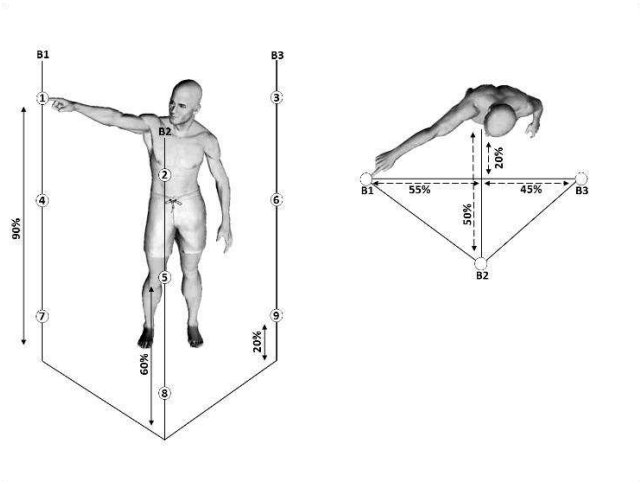


**Figure 1. Illustration of the experimental protocol. Placement of the nine targets on three supporting bars (B1, B2, B3, three targets on each vertical bar) is based on the subject's height (shown as percentages in figure). Subjects performed point-to-point movements between all pairs of targets (a total of 72 movements) and repeated each movement 30 times.**

## 2 EXPERIMENTAL PROCEDURES

### 2.1 Subjects

Four healthy right-handed participants (E1, E2, E3, E4, 2 males, aged = 25 ± 3 old) with no history of neuromuscular disease voluntarily participated in the experiment. The experiment conformed to the Declaration of Helsinki and written consent was obtained following guidelines of the Université de Bourgogne.

### 2.2 Task

Participants executed whole-body point-to-point movements in various directions at a self-selected pace. In brief, the experimental protocol (illustrated in Figure 1) specified 9 targets on 3 vertical bars. Each bar had 3 targets on different heights determined based on the participant's height. Participants stood barefooted and performed pointing movements between all pairs of targets (i.e. a total of 72 different pointing movements or "tasks") using the index fingertip of their dominant right arm.

### 2.3 EMG Recording and Preprocessing

We recorded the activity of 30 muscles by means of an Aurion (Milan, Italy) wireless surface EMG system. The skin was shaved before electrode placement, and abraded softly. EMG electrodes were placed symmetrically on the two sides of the body on the following muscles : tibialis anterior (Ta), soleus (So), peroneus (Pe), gastrocnemius (Ga), vastus lateralis (Vl), rectus femoris (Rf), biceps femoris (Bf), gluteus maximus (Gm), erector spinae (Es), pectoralis superior (Ps), trapezius (Tp), anterior deltoid (Da), posterior deltoid (Dp), biceps brachii (Bb), triceps brachii (Tb). We defined movement onset ($t_0$) and end ($t_{end}$) times as the times between which the fingertip velocity superseded 5% of its maximum and restricted our analysis to the interval ($t_0$- 100ms, $t_{end}$) of EMG activity. These movement-related EMGs for each trial were digitally full-wave rectified, low-pass filtered (Butterworth filter, cut-off frequency of 3Hz, zero-phase distortion) and normalized to 1,000 time steps. A final waveform of 50 time steps was then obtained by using trapezoidal integration of the latter signal on a uniform temporal grid. The EMG signal of each muscle was then normalized by dividing each single-trial muscle signal by its maximal value attained throughout the experiment.

## 3 DATA ANALYSIS & MODELING

### 3.1 Space-by-time Decomposition of Muscle Activity

We used a tensor decomposition [11] with non-negative constraints [12] to decompose the single-trial EMG signals into spatial and temporal synergies. This modularity model [13] represents muscle activity as a linear combination of separate but concurrent spatial and temporal synergies combined in single trials by scalar coefficients. According to the space-by-time factorization, a single-trial muscle pattern $M^l \in \mathbb{R}_+^{T \times M}$ can be written as a three-factor multiplication (T, M are the number of time frames and muscles):

$$M^l \simeq W_t A^l W_s, \quad \forall l \in [1, L] \qquad (1)$$

where $W_t \in \mathbb{R}_+^{T \times K}$ is a matrix whose columns are the temporal synergies, $W_s \in \mathbb{R}_+^{N \times M}$ is a matrix whose rows are the spatial synergies and the matrix $A^l = (a_{i,j}^l)_{1 \le i \le K, 1 \le j \le N}$ includes all single-trial activation coefficients. The parameters K and N correspond to the number of temporal and spatial synergies respectively and are free parameters of the decomposition model. Note that the matrices $W_t$ and $W_s$ are inferred from all trials, thus are independent of any particular trial, and constitute the invariant

synergies and Al are the trial-dependent activation coefficients targets (i.e. a total of 72 different pointing movements or "tasks") using the index fingertip of their dominant right arm.

## 3.2 Variance Accounted For

To assess how well the space-by-time decomposition reconstructed the original EMG recordings, we computed the Variance Accounted For (VAF) by the decomposition [7, 14]. VAF is a measure of goodness of fit and is defined as the total approximation error divided by the total variance of the dataset:

$$VAF = 1 - \frac{\sum_l \left\| M^l - W_t A^l W_s \right\|^2}{\sum_l \left\| M^l - \mathbf{m} \right\|^2} \quad (2)$$

The total approximation error is computed as the squared Frobenius norm (‖.‖) of the difference between the original muscle activity and its approximation by the space-by-time decomposition and the total variance of the dataset is the squared Frobenius norm of the difference between the original muscle activity and the mean EMG activation across all trials (**m**).

## 3.3 Synergy Extraction

To identify spatial synergies, temporal synergies and single-trial activation coefficients from the recorded muscle activity, we applied sNM3F, a NMF-based synergy extraction algorithm. sNM3F implements the space-by-time decomposition, i.e. identifies spatial and temporal components as well as activation coefficients that describe the performed movements [13, 15]. The advantage of NMF-based decompositions over other dimensionality reduction methods (e.g. PCA, ICA) is that they restrict the extracted synergies and activations to be non-negative, which makes them physiologically relevant for EMG signals as muscles cannot be activated "negatively".

## 3.4 Task Parameters

Our experimental design specified 9 targets placed on 3 different heights of 3 vertical bars (see 1 for an illustration), which defined 72 distinct pointing movements. Each of these movements can be fully described by the starting target (P1,...,P9) and end target (P1,...,P9) of the corresponding movement. Here, to characterize separately the temporal and spatial dimensions of the task at hand, we defined two groupings of the task parameters. The first grouping carried the temporal information of the task and consisted of parameters describing: a) the beginning of the movement (starting target, bar and height), b) the transient movement phase (direction, horizontal direction and vertical direction) and c) the movement end (end target, bar and height). The second grouping carried the spatial information of the task describing: a) the horizontal dimension of movement (starting bar, horizontal direction, end bar) and b) the vertical dimension of movement (starting height, vertical direction, end height) independently of the timing.

## 3.5 Decoding Task Parameters

The activation coefficient $a_{i,j}^l$ represents the relative amplitude of temporal synergy i in the muscles defined by spatial component j on trial l. Thus, the activation coefficients can be used as the single-trial parameters that relate each synergy to the movement performed in each trial or the task parameters characterizing the trial. Hence, to test if the space-by-time synergy recruitment allows decoding task parameters, we employed a single-trial classification analysis that used as parameters the activation coefficients $A^l$ . In particular, we used a linear discriminant analysis (LDA) in conjunction with leave-one-out cross-validation and quantified decoding performance as the percentage of correctly decoded trials [7, 16-18].

## 3.6 Confusion Matrices

To illustrate which task parameters are discriminated reliably and which are typically confused, we reported decoding results in the form of confusion matrices. The values on a given row i and column j of a confusion matrix D(i, j) report the fraction of trials in which we decoded a value j of a task parameter while the actual value of this parameter in that trial was i. Hence, the confusion matrices illustrate not only the percentage of correctly decoded trials but also the distribution of decoding errors, thereby showing which combination of parameters tend to be confounded.

## 3.7 Selecting the Number of Synergies

We employed the decoding analysis described above to identify the most compact and task-discriminating space-by-time decomposition. We increased gradually the numbers of temporal and spatial synergies extracted (K, N respectively) and decoded the motor task performed on each trial for each N × K-dimensional decomposition. The optimal number of synergies was then selected as the step at which adding any supplementary synergy did not give any significant gain in task decoding performance ($p > 0.05$).

## 3.8 Clustering Synergies based on their Functional Similarity

We propose a novel method for clustering synergies across participants based on their functional similarity as revealed by the task decoding analysis. Typically in motor modularity studies, synergies are clustered using as criterion their activation similarity, i.e. temporal (spatial) synergies belong to the same cluster if they have similar temporal activation profiles (muscle activations) [19, 20]. However, several factors, including individual idiosyncracies, motor choices and physiological differences, may lead to different muscle groupings and/or temporal activations, whereas the underlying synergies may have the same functionality with respect to task performance. Hence, here we propose clustering synergies of the same type (spatial or temporal) across participants based on whether they allow decoding the same task features.

In the following, we present the clustering of spatial synergies (Fig. 2). First, using the LDA approach we described above, for each spatial synergy of the N spatial synergies we computed the 72 × 72 confusion matrix showing how well it decodes the 72 performed movements. Then, as similar confusion matrices reveal similar

coding of task parameters, we grouped synergies using as clustering measure the similarity of their confusion matrices. We reshaped each confusion matrix as a 5184-dimensional vector and computed the correlation coefficient ($r_{i,j}$) between all such pairs of vectors (corresponding to pairs of temporal synergies) across all pairs of participants. This procedure yielded an N × N lower triangular matrix, each entry of which represents the functional similarity of each pair of synergies. Then, using $r_{i,j}$ as distance measure, we input all synergies from all participants to an agglomerative hierarchical clustering algorithm [44]. The algorithm created a hierarchical cluster tree from all synergy pairs (using as distance between two clusters the furthest distance between all pairs of objects across the two clusters, [31]). The hierarchical trees for the temporal and spatial synergies are shown in Figure 5 top.

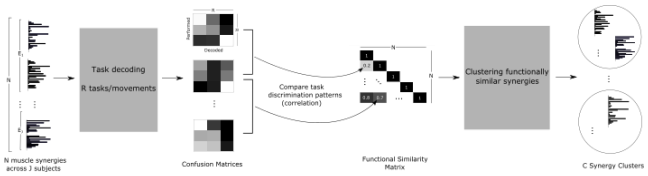


**Figure 2. Schematic illustration of our computational approach comprising decoding, functional similarity analysis and clustering. We input the single-trial activations of each of the N muscle synergies to a decoding algorithm that predicts which of the R movements was performed on each trial. We plot the results in the form of R × R confusion matrices. Then we compare the confusion matrices of all synergies by computing their pairwise correlations and summarizing them in a N × N lower triangular functional similarity matrix. Finally, we use a hierarchical clustering algorithm to group similar synergies onto C distinct clusters.**

# 4 RESULTS

## 4.1 Space-by-time modular decomposition of whole-body muscle activity

We applied the sNM3F algorithm to the (pre-processed) EMG recordings of each participant to extract a space-by-time representation of the single-trial muscle activity during performance of the 72 distinct whole-body pointing movements defined in the experimental protocol. We found that the EMG patterns of all four participants were composed of four temporal synergies (K = 4), whereas a different number of spatial synergies was identified across participants (E1: N = 4, E2: N = 6, E3: N = 7, E4: N = 5). To evaluate the plausibility of the resulting space-by-time decompositions, we quantified a) how well they approximate the original EMG recordings and b) how well they discriminate in single trials the 72 performed movements. We found that the identified decompositions achieved on average across subjects (mean ± sem) a VAF value of 68%±5% and decoding performance of 86%±1%.

The temporal synergies of the space-by-time decomposition are time-varying patterns of muscle activity representing the stereotypical temporal profiles of activations shared across muscles. The four temporal synergies extracted from the data of an example participant are shown in Figure 3A. Each synergy represents a burst of muscle activity and the four bursts are consecutive in time spanning the whole movement duration.

The spatial synergies are vectors of muscle activity levels representing fixed balances of muscle activations at any point in time. The five spatial synergies of the example participant are shown in Figure 4A. Each synergy comprises activation of muscles over the entire body including upper and lower limbs and both hemibodies. Hence, the extracted spatial synergies do not separate specific body parts which suggests that they represent functional groupings of muscle activations rather than purely anatomical constraints or couplings resulting from crosstalk from neighboring muscles in EMG recordings.

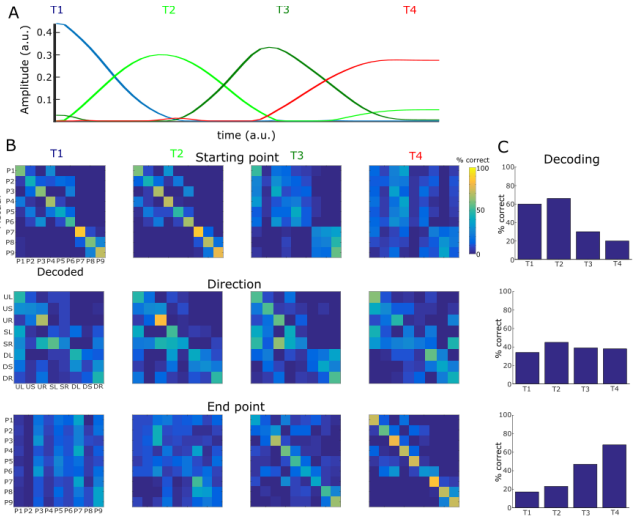


**Figure 3. Task coding function of temporal muscle synergies. A. The four temporal synergies extracted from the single-trial EMG data of an example subject. The four synergies are successive in time covering the full movement duration. B. Confusion matrices illustrating how well each one of the four temporal synergies (organized in rows) can discriminate the starting point (top), direction (middle) and endpoint of the movement. C. Percentages of correct decoding of each "temporal" task parameter (starting point, direction & endpoint) by each of the temporal synergies.**

## 4.2 Functional role of temporal muscle synergies

We next investigated what aspects of the task are described by the activation of temporal synergies. To this end, we performed decoding analyses, i.e. we used the activation coefficients combining each temporal synergy with all spatial synergies to decode task parameters and plotted the results in the form of confusion matrices.

Single-trial activations of the first temporal synergy characterize the movement starting point (P1,...,P9, 60% correct decoding - chance level is 11% for all 9-wise discriminations performed in this, see top left confusion matrix in Fig. 3B). The second temporal

synergy also describes the starting target (66% correct decoding, 1.81 bits - 57%) as well as the movement direction (45% correct decoding). Interestingly, the second synergy decoded the starting target better than the first synergy, probably because the first synergy captures mainly tonic (postural) muscle activity whereas the second one describes movement initiation, which has typically higher signal-to-noise ratio. The third temporal synergy also contributes to the discrimination of the movement direction (39% correct decoding) by discriminating mostly the downward movements (72% correct decoding) from all others. It also distinguishes partly the end target (47% correct decoding), though the end target is decoded best by the fourth temporal synergy (68% on average, 76% correct decoding of end height, 78% correct decoding of end bar).

Taken together, these results suggest that the four temporal synergies of muscle activity correspond to four different phases of goal-directed voluntary movement. Thus, this specific temporal structure of muscle activity serves to convey complementary task information in time in order to characterize the movement evolution from the starting point to the endpoint.

## 4.3 Functional role of spatial muscle synergies

Following the functional characterization of the temporal synergies, we performed a similar decoding analysis in the spatial dimension to investigate which task parameters are encoded by the activations of spatial synergies. Unlike temporal synergies that characterized all temporal task features in distinct movement phases, activations of each spatial synergy described a distinct subset of spatial task features in the entire movement duration. In particular, we identified spatial synergy activations that explain differences in the vertical dimension of movement (the first, second & fifth synergies shown in Fig. 4A) and others that explain differences in the horizontal dimension (the third & fourth synergies shown in Fig. 4A). We also note that the task decoding contributions of the spatial synergies are not as distinct as for the temporal synergies (see similar task decoding scores across synergies in Fig. 4C). Nevertheless, although all synergies provide information about the task, there is a consistent distinction between synergies decoding mainly the vertical dimension of motion and others that decode the horizontal dimension.

We also investigated how well the spatial modules discriminated the temporal task variables and vice-versa. This served as a direct comparison between temporal and spatial modules in order to dissociate their respective functional roles. We found that considerably less spatial (temporal) task information was conveyed by temporal (spatial) modules (for comparison, spatial modules carried 0.79 to 1.19 bits about the starting target, 0.52 to 0.66 bits about the movement direction and 0.48 to 1.29 bits about the end target).

Overall, similarly to the temporal synergies, the spatial synergies serve distinct motor functions that can be explained in terms of their muscle composition. In contrast to the temporal synergies that relate to temporal task features, the structure and shape of the spatial synergies relate task parameters pertaining to the spatial dimension of motion (either vertical or horizontal) over the full time-course of movement. Importantly, when combining all spatial and temporal synergies, sufficient task information is conveyed to allow unequivocal characterization of the movement performed on each trial (85% correct decoding across the 72 movements).

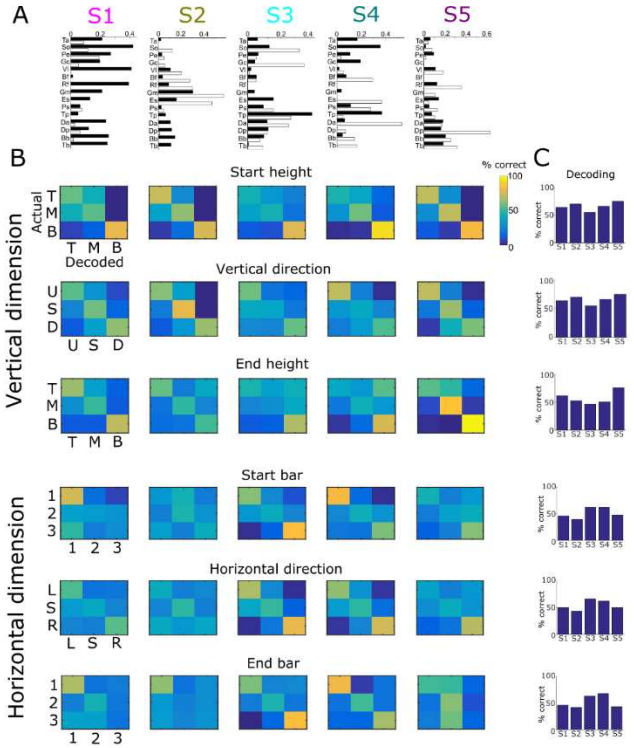


**Figure 4. Task coding function of spatial muscle synergies. A. The five spatial synergies extracted from the single-trial EMG data of an example subject as vectors of muscle activation levels (left hemibody muscles shown in white and right hemibody muscles in black). B. Confusion matrices illustrating how well each one of the five spatial synergies (organized in rows) can discriminate task parameters describing the vertical dimension of movement (top three rows - starting height, vertical direction and end height) and the horizontal dimension of movement (bottom tree rows - starting bar, horizontal direction and end bar). C. Percentages of correct decoding of the "spatial" task parameters by the five spatial synergies.**

## 4.4 Functionally similar muscle synergies across subjects

After characterizing the modular organization of muscle activity for the example subject, we examined whether the same structure holds for the muscle activity of all four participants we tested. To do this, we implemented a clustering procedure to group the extracted synergies of all participants based on the similarity of their movement decoding confusion matrices.

We found three clusters of temporal synergies and three clusters of spatial synergies. Figure 5A-B shows the hierarchical trees obtained from the hierarchical clustering algorithm as well as the functional similarity matrices for the temporal and spatial synergies

respectively (clusters are color-coded). Although clustering was based solely on task decoding results, the three resulting temporal clusters (blue, green and red) contained synergies with similar activations in time (early, transient and late activations respectively), which indicates that the functional role of temporal synergies is highly related to their temporal occurrence. Regarding the spatial synergies, three clusters (cyan, purple and yellow) were formed all containing synergies across different subjects. Our clustering analysis also specified a few spatial synergies that were functionally dissimilar to others (shown in black in Fig. 5) and were not included in the clusters.

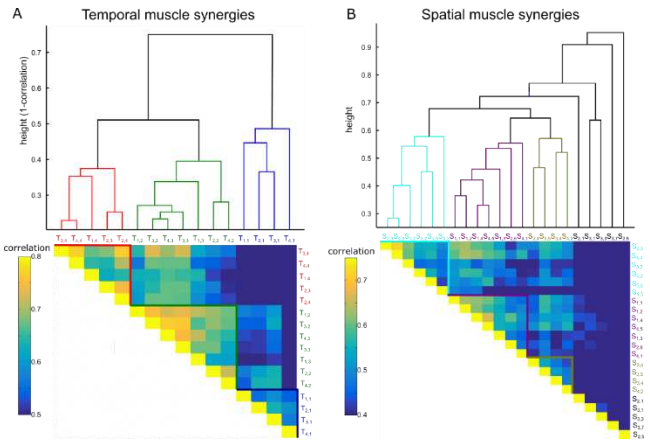


**Figure 5. Hierarchical cluster trees and the corresponding functional similarity matrices for the temporal muscle synergies (A) and the spatial muscle synergies (B) across all subjects. Synergy $T_{a,b}$ represents the bth temporal synergy (S for spatial synergies) of subject a. Color-coded branches of the hierarchical trees represent synergies that are clustered together based on the correlation of their confusion matrices. Pairwise correlation of the confusion matrices of synergies i and j is shown as entry (i, j) of the functional similarity matrix.**

## 5 DISCUSSION

In this study, we linked temporal and spatial muscle synergies to task parameters and derived a task representation interpretation of modular muscle activity in a whole-body pointing task. Our findings indicate that motor signals have a low-dimensional structure based on the combined activations of a) temporal synergies that encode distinct movement phases (initiation, transient or termination) and b) spatial synergies that encode distinct 3-dimensional spatial directions between initial and final positions. Crucially, both types of synergies capture complementary, not redundant nor irrelevant, aspects of the task over time and space. Finally, by introducing a novel functional similarity analysis, we identified a small set of temporal and spatial synergies that, despite differences in their activation profiles, had synergistic functional roles in movement execution consistently amongst participants.

### 5.1 From Task Parameters to Muscle Activations and Vice-versa

Our findings are compatible with a hierarchical organization of motor signals for the production of muscle patterns that are effective in task space [21-24]. Hence, spatial and temporal muscle synergies may represent the pivot of such a hierarchical neural control structure in which higher-level brain circuits operate on task-related variables and lower-level circuits construct full muscle activities by combining descending motor commands with reflex contributions to effectively produce movements.

### 5.2 Task Relevance of Muscle Synergies

An important contribution of our study is the dissociation of the roles of the identified neural/kinematic patterns. This was only made possible by the joint cognitive modeling of behavioral and neural/kinematic data that linked the neural correlates of sensori-motor behavior with the higher cognitive processes involved in decision-making. Similar model-based cognitive neuroscience approaches have been proposed recently and have been shown to be effective in characterizing the neural underpinnings of behavioral components [32]. Here we found that the subjects' cognitive state on each trial - as reflected by trial-to-trial variability of the brain-behavior coupling in a) occipital and b) prefrontal cortices – indexes the reliability of a) sensory encoding and b) integration of perceptual information.

### 5.3 Clusters of Functional Muscle Synergies

A corollary of the current study is the proposal of a "functional similarity" approach aiming to cluster synergies from different subjects that have similar functional roles as represented by the task parameters they encode. This observation motivated the necessity of new methodologies to assess synergy similarity across humans and enhance personalization of treatments. Our approach opens up new perspectives for matching synergies across individuals, which may find applications in therapeutic/rehabilitation research.

## REFERENCES

[1] Bizzi, E., Cheung, V.C., d'Avella, A., Saltiel, P., and Tresch, M. (2008). Combining modules for movement. Brain Res Rev 57, 125-133.

[2] d'Avella, A., Saltiel, P., and Bizzi, E. (2003). Combinations of muscle synergies in the construction of a natural motor behavior. Nat Neurosci 6, 300-308.

[3] Tresch, M.C., Saltiel, P., and Bizzi, E. (1999). The construction of movement by the spinal cord. Nat Neurosci 2, 162-167.

[4] Delis, I., Chiovetto, E., and Berret, B. (2010). On the origins of modularity in motor control. J Neurosci 30, 7451-7452.

[5] Hart, C.B., and Giszter, S.F. (2010). A neural basis for motor primitives in the spinal cord. J Neurosci 30, 1322-1336.

[6] Berniker, M., Jarc, A., Bizzi, E., and Tresch, M.C. (2009). Simplified and effective motor control based on muscle synergies to exploit musculoskeletal dynamics. Proc Natl Acad Sci U S A 106, 7601-7606.

[7] Delis, I., Berret, B., Pozzo, T., and Panzeri, S. (2013). Quantitative evaluation of muscle synergy models: a single-trial task decoding approach. Front Comput Neurosci 7, 8.

[8] Todorov, E., Li, W., and Pan, X. (2005). From task parameters to motor synergies: A hierarchical framework for approximately-optimal control of redundant manipulators. J Robot Syst 22, 691-710.

[9] Hug, F., Turpin, N.A., Guevel, A., and Dorel, S. (2010). Is interindividual variability of EMG patterns in trained cyclists related to different muscle synergies? J Appl Physiol (1985) 108, 1727-1736.
[10] Frere, J., and Hug, F. (2012). Between-subject variability of muscle synergies during a complex motor skill. Front Comput Neurosci 6, 99.
[11] Cichocki, A., Mandic, D.P., Phan, A.H., Caiafa, C.F., Zhou, G.X., Zhao, Q.B., and De Lathauwer, L. (2015). Tensor Decompositions for Signal Processing Applications. Ieee Signal Proc Mag 32, 145-163.
[12] Cichocki, A., Zdunek, R., and Amari, S.I. (2008). Nonnegative matrix and tensor factorization. Ieee Signal Proc Mag 25, 142-145.
[13] Delis, I., Panzeri, S., Pozzo, T., and Berret, B. (2014). A unifying model of concurrent spatial and temporal modularity in muscle activity. Journal of Neurophysiology 111, 675-693.
[14] d'Avella, A., Portone, A., Fernandez, L., and Lacquaniti, F. (2006). Control of fast-reaching movements by muscle synergy combinations. J Neurosci 26, 7791-7810.
[15] Delis, I., Panzeri, S., Pozzo, T., and Berret, B. (2015). Task-discriminative space-by-time factorization of muscle activity. Frontiers in Human Neuroscience 9.
[16] Delis, I., Berret, B., Pozzo, T., and Panzeri, S. (2013). A methodology for assessing the effect of correlations among muscle synergy activations on task-discriminating information. Front Comput Neurosci 7, 54.
[17] Delis, I., Chen, C., Jack, R.E., Garrod, O.G.B., Panzeri, S., and Schyns, P.G. (2016). Space-by-time manifold representation of dynamic facial expressions for emotion categorization (vol 16, 14, 2016). J Vision 16.
[18] Delis, I., Onken, A., Schyns, P.G., Panzeri, S., and Philiastides, M.G. (2016). Space-by-time decomposition for single-trial decoding of M/EEG activity. NeuroImage 133, 504-515.
[19] d'Avella, A., and Bizzi, E. (2005). Shared and specific muscle synergies in natural motor behaviors. Proc Natl Acad Sci U S A 102, 3076-3081.
[20] Torres-Oviedo, G., and Ting, L.H. (2010). Subject-specific muscle synergies in human balance control are consistent across different biomechanical contexts. J Neurophysiol 103, 3084-3098.
[21] McKay, J.L., and Ting, L.H. (2012). Optimization of muscle activity for task-level goals predicts complex changes in limb forces across biomechanical contexts. PLoS Comput Biol 8 (4), e1002465.
[22] Ting, L.H., and McKay, J.L. (2007). Neuromechanics of muscle synergies for posture and movement. Curr Opin Neurobiol 17, 622-628.
[23] Tresch, M.C. (2007). A balanced view of motor control. Nat Neurosci 10, 1227-1228.
[24] Tresch, M.C., and Jarc, A. (2009). The case for and against muscle synergies. Curr Opin Neurobiol 19, 601-607.